ASYMMETRIC RECTANGULAR OBSTRUCTION THERMAL EFFECTS ON ENTRANCE REGIONS OF FLAT PLATE CHANNELS

Aldélio Bueno Caldeira
Instituto Militar de Engenharia, Departamento de Engenharia Mecânica e de Materiais - 22290-270 – Rio de Janeiro – RJ - Brazil
aldelio@ime.eb.br

Albino José Kalab Leiroz
Universidade Federal do Rio de Janeiro, Programa de Engenharia Mecânica - 21945-970 – Rio de Janeiro - RJ - Brazil
leiroz@ufrj.br

Helcio Rangel Barreto Orlande
Universidade Federal do Rio de Janeiro, Programa de Engenharia Mecânica - 21945-970 – Rio de Janeiro - RJ - Brazil
helcio@serv.ufrj.br

Abstract. *Conjugate thermal effects of asymmetric rectangular obstructions on entrance regions of parallel plate channels are numerically investigated in the present work. The incompressible laminar flow governing equations, written in vorticity-stream function formulation, as well as the energy conservation equation are discretized with a WUDS finite difference/ volume scheme. The domain is subdivided into zones and a regular mesh is used within the obtained subdomains. Constant temperature boundary conditions are considered in the present study for the channel walls. Results are obtained for fully developed and uniform inlet velocity profiles. The effects of the obstruction asymmetry on the temperature field and Nusselt number are analyzed. The numerical results obtained here are validated with limiting analytical solution available in the literature.*

Keywords. *conjugate heat transfer, rectangular obstruction, entrance region, parallel flat plate.*

1. Introduction

The study of internal convection effects within parallel plate channels share the interest of basic and applied research. The design and development of flame holders for combustion devices (Williams, 1985, and Esquiva-Dano et al., 2001, Hanff and Campbell, 2002), the cooling of electronic systems (Davallah and Bayazitoglu, 1987, Desrayaud et al., 2002), fouling and fins in heat exchangers (Kern, 1965) and thermal intrusive aspects of measurement devices (Holman, 1989) are among the applications motivating the study of the rectangular obstructions inside parallel plate channel. Furthermore, the works on conjugate heat transfer reveal important physical phenomena as the reverse heat transfer (Andrade and Zaparoli, 1999).

The effects of rectangular obstructions inside parallel plate channels on entrance regions was numerically studied by Caldeira et al. (2001). The objective was modeling the intrusive aspects of orifice plate devices into thermal and fluid flow. The influence of Reynolds number, obstruction thickness, height and asymmetry, considering constant wall temperature or heat flux boundary conditions were evaluated. The results showed that there was a strong relationship between the eddy zones and the heat transfer phenomena, based on the Nusselt number behavior along the channel and obstruction walls. Conjugate heat transfer was not considered in that work.

The conjugate heat transfer effects of a symmetric rectangular obstruction on the hydrodynamical and thermal entrance regions within parallel plate channels were studied by Caldeira et al. (2002). The rectangular obstruction thermal effects were analyzed using the temperature field and the Nusselt number evaluated along the channel and obstruction walls. Heat transfer enhancement due to the obstruction, which presents an internal fin effect, and the conduction heat transfer within the obstruction were shown. The laminar incompressible flow governing equations were written in vorticity-stream function approach. Constant wall temperature and constant wall heat flux boundary conditions were considered for the channel walls. The physical solution domain was divided into five subdomains. Numerically, the finite difference method was used with an implicit hybrid scheme. The solutions were obtained employing an iterative procedure applied inside each subdomain. In other words, the systems of algebraic equations were not simultaneously solved for all domain, but for each subdomain in sequence.

In the present work, conjugate heat transfer effects of asymmetric rectangular obstruction on the fluid dynamic and thermal entrance regions within parallel plate channels are studied. The rectangular obstruction thermal effects are analyzed using the temperature field and the Nusselt number evaluated along the channel and obstruction walls. Heat transfer enhancement due to the obstruction and the conduction heat transfer within the obstruction are also analyzed. The laminar incompressible flow governing equations written in vorticity-stream function form are discretized with an implicit finite difference/ volume scheme. The physical solution domain is divided into five zones and regular discretizing grids are used within the obtained subdomains. The resulting systems of algebraic equations are solved simultaneously in the domain. Constant temperature boundary conditions are considered for the channel walls. The Graetz problem (Kays and Crawford, 1980) is used to validate the obtained numerical results.

2. Mathematical Formulation

It is note worthy that the proposed physical-mathematical model only considers the heat transfer into the fluid and solid obstruction. So, the conduction through the channel walls is not taken into account in the present work.

The solution domain is depicted in Fig. (1), with the principal geometric dimensions, which also shows the Cartesian system of coordinates used in the present work.

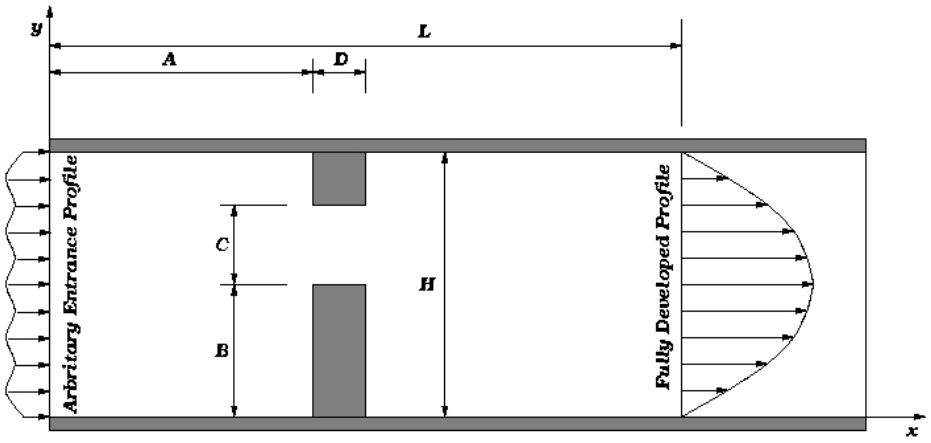

Figure 1. Physical domain and principal dimensions.

The dimensionless system of equations for the conservation of mass and *momentum,* for the fluid domain, considering laminar and incompressible flow inside the channel, and the energy, for the fluid and solid domains, are written as

$$\frac{\partial u_x}{\partial x}+\frac{\partial u_y}{\partial y}=0 \tag{1}$$

$$\frac{\partial u_x}{\partial t}+\frac{\partial u_x\,u_x}{\partial x}+\frac{\partial u_y\,u_x}{\partial y}=-\frac{\partial P}{\partial x}+\frac{1}{Re}\left(\frac{\partial^2 u_x}{\partial x^2}+\frac{\partial^2 u_x}{\partial y^2}\right) \tag{2}$$

$$\frac{\partial u_y}{\partial t}+\frac{\partial u_y\,u_x}{\partial x}+\frac{\partial u_y\,u_y}{\partial y}=-\frac{\partial P}{\partial y}+\frac{1}{Re}\left(\frac{\partial^2 u_y}{\partial x^2}+\frac{\partial^2 u_y}{\partial y^2}\right) \tag{3}$$

$$\frac{\partial \theta}{\partial t}+\frac{\partial u_x\,\theta}{\partial x}+\frac{\partial u_y\,\theta}{\partial y}=\frac{\partial}{\partial x}\left(D\frac{\partial \theta}{\partial x}\right)+\frac{\partial}{\partial y}\left(D\frac{\partial \theta}{\partial y}\right) \tag{4}$$

with boundary conditions

$$u_x=f_i(y),\quad u_y=0,\quad \theta=1;\quad x=0,\ 0\le y\le 1 \tag{5}$$

$$u_x=f_o(y),\quad u_y=0,\quad \partial\theta/\partial x=\partial\theta_w/\partial x;\quad x\to\infty,\ 0\le y\le 1 \tag{6}$$

$$u_x=0\ ,\ u_y=0\ ;\quad 0\le x\le\infty\ ;\quad at\quad h_l(x,y)\quad and\quad h_u(x,y) \tag{7}$$

$$a_l\,\theta+b_l\,\partial\theta/\partial y=\varphi_l;\quad 0\le x\le\infty\ ,\ y=0 \tag{8}$$

$$a_u\,\theta-b_u\,\partial\theta/\partial y=\varphi_u;\quad 0\le x\le\infty\ ,\ y=1 \tag{9}$$

The constants a_l, b_l, a_u, b_u, φ_l and φ_u appearing in Eq.(8-9) will be set accordingly with the kind of boundary condition being considered for each case.

The initial conditions are given by

$$u_x=0\ ,\ u_y=0\ ,\ \theta=0\quad ;\quad 0\le x<\infty\ ,\ 0<y<1 \tag{10}$$

The functions $h_l(x,y)$ and $h_u(x,y)$ appearing in Eq.(7) are used to describe the lower and upper irregular solid surfaces, being defined as

$$h_l(x,y)=\begin{cases} y=0; \quad 0 \le x < A/H \\ x=A/H; \quad 0 \le y \le B/H \\ y=B/H; \quad A/H < x < (A+D)/H \\ x=(A+D)/H; \quad 0 \le y \le B/H \\ y=0; \quad (A+D)/H < x < \infty \end{cases} \tag{11}$$

and

$$h_u(x,y)=\begin{cases} y=1; \quad 0 \le x < A/H \\ x=A/H; \quad (B+C)/H \le y \le 1 \\ y=(B+C)/H; \quad A/H < x < (A+D)/H \\ x=(A+D)/H; \quad (B+C)/H \le y \le 1 \\ y=1; \quad (A+D)/H < x < \infty \end{cases} \tag{12}$$

The dimensionless variables appearing in Eqs.(1-10) are defined as

$$x=\frac{X}{H};\ y=\frac{Y}{H};\ u_x=\frac{U_X}{U_{max}};\ u_y=\frac{U_Y}{U_{max}};\ p=\frac{P}{\rho(U_{max})^2};\ \theta=\frac{T_c-T}{T_c-T_i};\ t=\frac{t^*}{H/U_{max}} \tag{13}$$

where the channel height (H) and the maximum velocity at the outlet (U_{max}) are used as length and velocity characteristic quantities, respectively. The dimensionless temperature (θ) is defined in terms of a constant characteristic temperature, T_c, and of a constant inlet temperature, T_i. For the constant wall temperature case, T_c, is defined as the channel wall temperature value, T_w.

The dimensionless physical parameters of the system of equations are the Reynolds number (*Re*) and dimensionless diffusivity parameter (*D*). These parameters are defined as

$$Re=\frac{U_{max}\,H}{\nu}; \tag{14}$$

$$D=\begin{cases} D_f=\dfrac{\alpha}{U_{max}H} \\ D_s=\dfrac{\alpha_s}{U_{max}H} \end{cases} \tag{15}$$

where ν, α and α_s represent the kinematic viscosity, the fluid and solid thermal diffusivities, respectively. D_f is the reciprocal of the Peclet number and D_s is a dimensionless diffusivity parameter for the solid obstruction. Note that D_s is just introduced in order to maintain the same dimensionless space and time scales on the solid and fluid subdomains.

The flow governing equations are rewritten in dimensionless vorticity-stream function form as

$$\frac{\partial\xi}{\partial t}+\frac{\partial u_x\,\xi}{\partial x}+\frac{\partial u_y\,\xi}{\partial y}=\frac{1}{Re}\left(\frac{\partial^2\xi}{\partial x^2}+\frac{\partial^2\xi}{\partial y^2}\right) \tag{16}$$

$$-\xi=\frac{\partial^2\psi}{\partial x^2}+\frac{\partial^2\psi}{\partial y^2} \tag{17}$$

with boundary conditions

$$\psi = \int_0^y f_i(y)\,dy; \quad x = 0,\ 0 \le y \le 1 \tag{18}$$

$$\psi = \int_0^y f_o(y)\,dy; \quad x \to \infty,\ 0 \le y \le 1 \tag{19}$$

$$\psi = 0; \quad 0 \le x \le \infty \ , \quad at \quad h_l(x,y) \tag{20}$$

$$\psi = \int_0^1 f_i(y)\,dy; \quad 0 \le x \le \infty \ , \quad at \quad h_u(x,y) \tag{21}$$

and initial conditions

$$\psi = 0\ ,\ \xi = 0\ ;\ 0 \le x < \infty\ ,\ h_l(x,y) < y < h_u(x,y) \tag{22}$$

Vorticity (ξ) and stream function (ψ) are respectively defined in terms of the longitudinal and transversal velocity components as

$$\xi = \frac{\partial u_y}{\partial x} - \frac{\partial u_x}{\partial y} \tag{23}$$

and

$$u_x = \frac{\partial \psi}{\partial y}, \quad u_y = -\frac{\partial \psi}{\partial x} \tag{24}$$

The vorticity values along the solid boundaries and at the channel inlet and outlet are initially unknown. These quantities are determined by an iterative solution procedure of the flow equations, which also accounts for the treatment of the non-linear terms appearing in Eq. (16) (Anderson et al., 1984).

3. Numerical Aspects

In the present work, the finite differences/ volumes method was used for the numerical solution of the governing equations previously described. The semi-infinite physical domain was truncated at $x = L / H$ where the outlet boundary conditions were applied. Numerical tests were performed for different values of L in order to guarantee independence of the truncated domain length. The truncated domain length was considered satisfactory when the deviation between the numerical Nusselt number in the end of the channel and the analytical Nusselt number (Kays and Crawford, 1980*)* for thermal developed flow were smaller than *1%*. The WUDS (Raithby and Torrance, 1974) is used as the interpolation function in an implicit scheme. The linear systems of equations are solved by the GMRES algorithm (Press et al. 1992). Furthermore, despite the transient nature of equations being solved, only the steady state results were analyzed in the present work. The half volume approach is employed in the boundaries as in the finite difference method, becoming easier the use of the first kind boundary conditions for the temperature, vorticity and stream function. In the interior volumes of the domain the finite volume method is used. In the solid obstruction/ fluid interface, the centers of the volumes are on the interface. On these interfaces parts of the volumes are in the solid and parts of the volumes are in the fluid. In the solid domain the velocity is prescribed null.

Regularly spaced points were used within the domain, defining the discretizing grid. The resulting system of algebraic equations was solved simultaneously for each partial differential equation discretized. In order to address the unknown vorticity values along the solution domain boundaries, an iterative procedure was employed. Initially, estimated vorticity values along the boundary were defined, allowing the solution of the vorticity transport equation, Eq. (16). With the obtained results, Eq. (17) was solved leading to the stream function distribution within the domain. Applying the velocity boundary conditions, stream function, vorticity and the definitions in terms of the primitive variables, a vorticity distribution along the solid boundaries was calculated. The obtained results allow the validation or correction of the initially estimated vorticity values. The iterative procedure was repeated until a specified tolerance criterion was satisfied. The solution was then marched in time.

The numerical solution proceeds until the obtained vorticity and temperature fields for two consecutive time steps differ by an amount smaller than a given steady state tolerance.

The Nusselt number along the channel walls is defined in terms of the dimensionless quantities by

$$Nu_l = \frac{2}{\theta_b - \theta_{w_l}} \frac{\partial \theta}{\partial y}\bigg|_{y=h_l} \tag{25}$$

$$Nu_u = \frac{2}{\theta_b - \theta_{w_u}} \frac{\partial \theta}{\partial y}\bigg|_{y=h_u} \tag{26}$$

where the dimensionless bulk temperature θ_b is defined by

$$\theta_b = \frac{\int_{h_l}^{h_u} (\theta\, u_x)\, dy}{\int_{h_l}^{h_u} u_x\, dy} \tag{27}$$

and the subscript (and sub-subscript) u and l are, respectively, associated with the upper and the lower solid wall.

4. Results

The analytical solution of Kays and Crawford (1980), considering constant temperature in the channel walls, for the Graetz problem is used to validate the proposed numerical procedure. Graetz problem consider a fully developed velocity and a developing temperature profiles inside parallel plate channels without obstructions. The formulation described by the Eqs. (1-10) leads to the Graetz problem formulation as the rectangular obstruction height, or thickness, vanishes. Inlet and outlet velocity profiles were defined as $f_i(y) = 4y - 4y^2$ and $f_o(y) = 4y - 4y^2$, respectively. Constant wall temperature, or first kind, ($a_u = a_l = 1, b_u = b_l = 0, \varphi_l = \varphi_u = \theta_w = 0$) thermal boundary conditions were considered. For the present analysis, the inlet and outlet temperature profiles were considered as uniform and fully developed, respectively.

Table (1) shows the comparison between the present numerical results for the Nusselt number along the channel wall for the Graetz problem with the analytical results of Kays and Crawford (1980), considering the cases of the first kind boundary conditions. Deviations smaller than *1%* between the numerical and analytical results are observed in Tab. (1).

Table 1. Nusselt number in the thermal developing region of the Graetz problem.

	Nu (θ_w = 0, *Re* = 100, D_f = 0.01, D_s = 0.01)	
x	*Numerical*	*Kays and Crawford, 1980*
4/3	*8.62*	*8.52*
8/3	*7.78*	*7.75*
20/3	*7.56*	*7.55*
∞	*7.55*	*7.54*

The numerical results presented in Tab (1) were obtained by using a grid with *481* and *41* points along the *x* and *y* directions, respectively and L/H equal to 12.

Results obtained for asymmetrical rectangular obstruction are shown below. The geometric and physical parameters for a base case are shown in Tab (2). The base case considers the uniform velocity profile at the channel inlet and the constant channel wall temperature. The cases analyzed in this work consider the base case parameter unless the specified ones in each case.

Table 2. Geometric and physical parameters for a base case.

Geometric Parameters				*Physical Parameters*		
A/H	*B/H*	*C/H*	*D/H*	*Re*	D_f	D_s
2	*0.7*	*0.3*	*0.3*	*100*	*0.01*	*0.01*

Figures (2-4) show the effect of the asymmetry of the obstruction on the flow field results. Comparing the Figs. (2-4) it is possible to observe, qualitatively, the dimension of the eddy zones. These zones increase with the obstruction

asymmetry. In Fig. (2), the analyzed case with greatest asymmetry, a single eddy zone with a large length is formed behind the obstruction. Otherwise, in Figs. (3) and (4) two eddy zones are presented behind the obstructions. The Fig. (3) shows a case with small obstruction asymmetry (*B/H = 0.4*) and the Fig. (4) shows a symmetric case (*B/H = 0.35*). The stream function field presented in fig. (3) reveals a significant asymmetry in the flow. So, small obstruction asymmetry can result in a great asymmetry in the flow field.

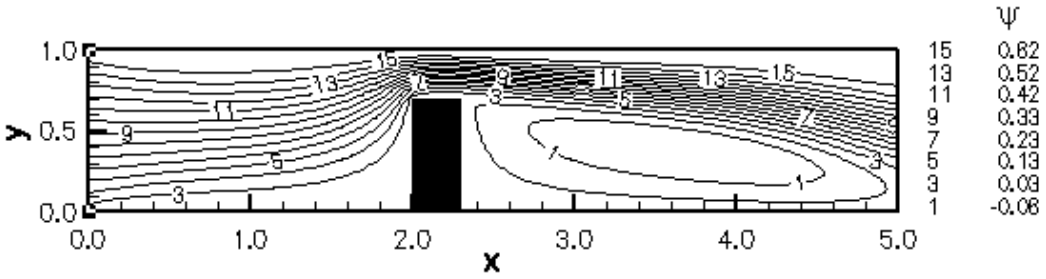

Figure 2. Stream function for the base case.

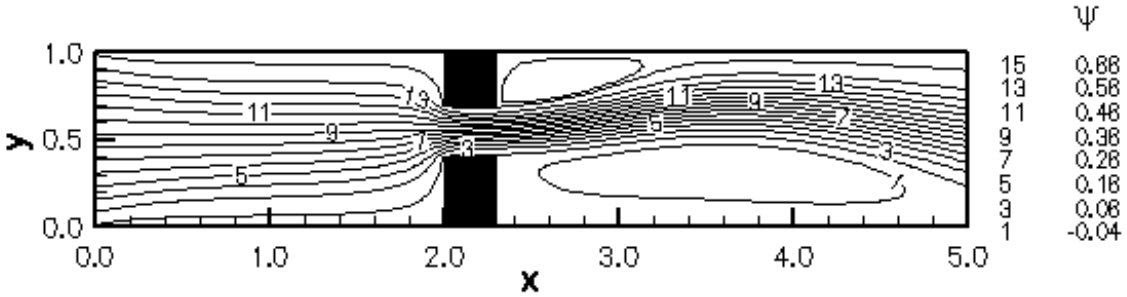

Figure 3. Stream function for the case with the same physical parameters of the base case and with the following geometric parameters: *A/H = 2, B/H = 0.4*, *C/H = 0.3* and *D/H = 0.3*.

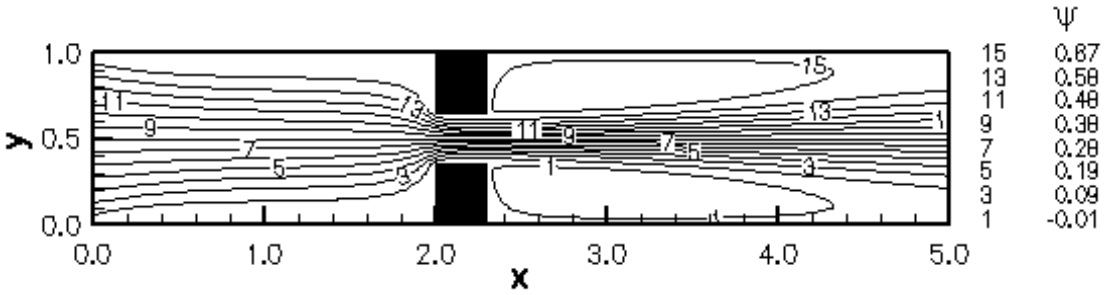

Figure 4. Stream function for the case with the same physical parameters of the base case and with the following geometric parameters: *A/H = 2, B/H = 0.35*, *C/H = 0.3* and *D/H = 0.3* (symmetric case).

The effects of the obstruction asymmetry on the temperature field are shown in Figs. (5-7). Observing the Figs. (2-7) is possible to identify the connection between the intensity of the eddy zones, behind the obstructions, and the coldest zones of the temperature field. The regions with low values of temperature increase into the fluid domains with the dimension of the obstruction, because of the improvement of the diffusion in eddy zones and of the greater heat transfer areas at obstruction/ fluid interface. Furthermore, increasing the obstruction asymmetry the hottest region is held in shorter lengths of the channel.

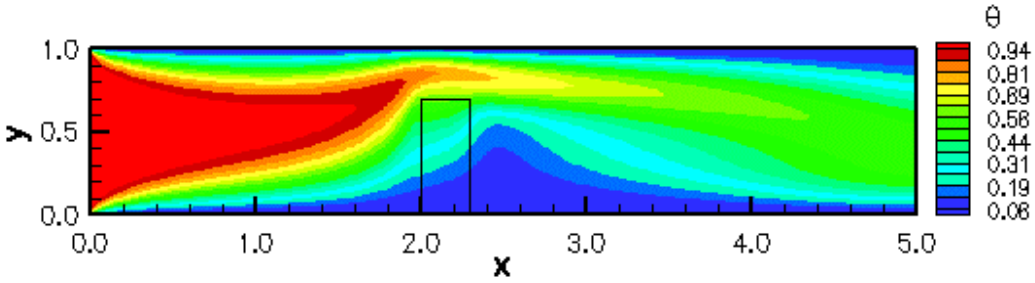

Figure 5. Temperature field for the base case.

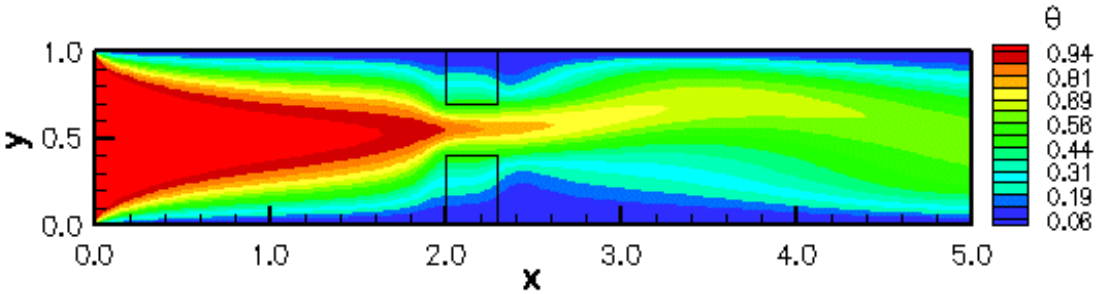

Figure 6. Temperature field for the case with the same physical parameters of the base case and with the following geometric parameters: *A/H = 2, B/H = 0.4*, *C/H = 0.3* and *D/H = 0.3*.

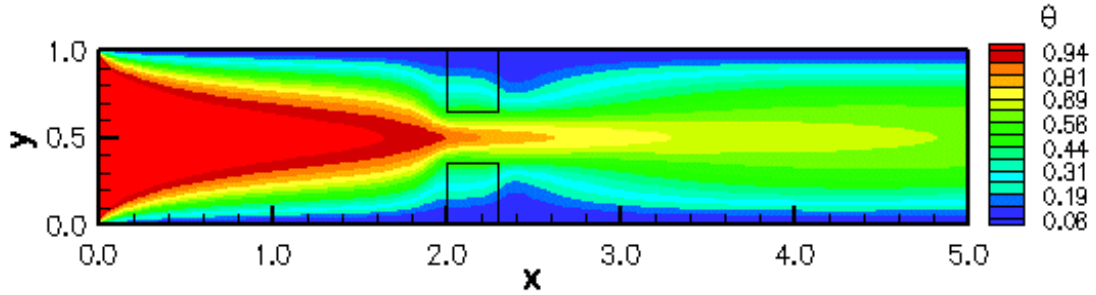

Figure 7. Temperature field for the case with the same physical parameters of the base case and with the following geometric parameters: *A/H = 2, B/H = 0.35*, *C/H = 0.3* and *D/H = 0.3* (symmetric case).

Figure (8) shows the Nusselt number behavior on the lower (Fig. (8a)) and upper (Fig. (8b)) solid walls for the cases with different asymmetric obstructions. For all cases, the thermal effects of the obstructions are represented by an abrupt increase of the Nusselt number at the inlet throat position. The increase of *Nu* is associated with the higher velocities and temperature gradients present inside the throat, improving the heat transfer by the convection mechanism. Downstream of the obstruction an abrupt decrease of *Nu* is also observed. Prior to abrupt increase, a reduction is also observed on *Nu* as the axial velocity decreases and a consequential weakening of convective effects follows. The reduction of *Nu* is associated with the eddy zones and the broadening of the thermal boundary layer. In Fig. (8a) high values of Nu_l are shown for the base case on the obstruction. Comparing the results for the asymmetrical and symmetrical cases within the downstream region, an overshooting of Nu_l values can be observed. The Nu_l overshooting increases with the eddy zone length.

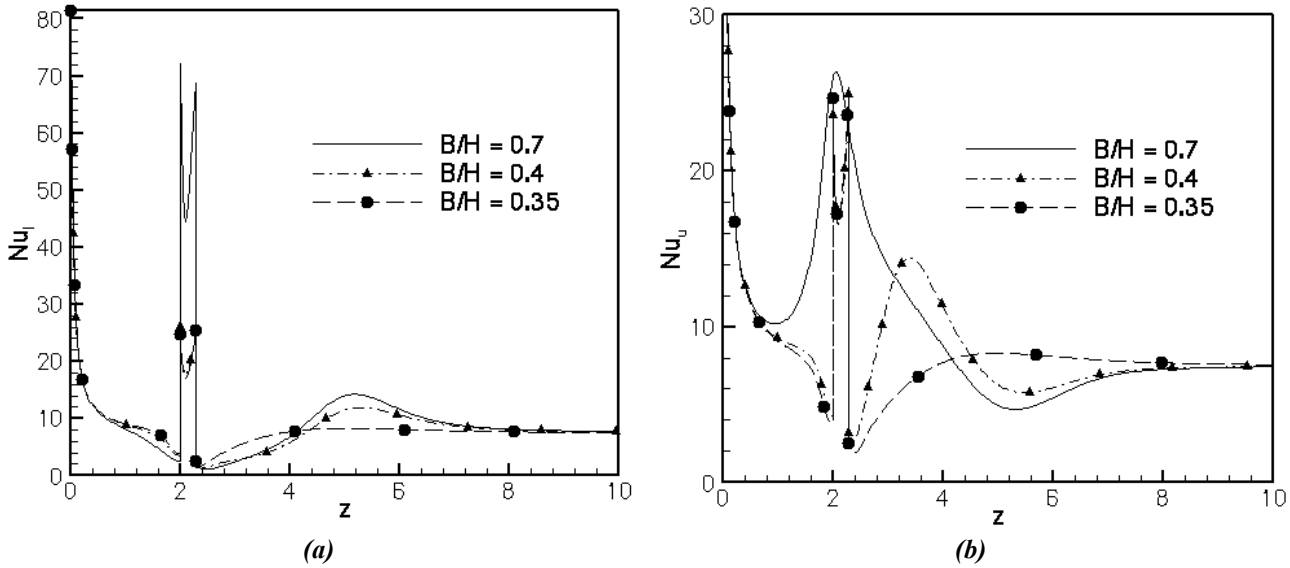

Figure 8. Asymmetry obstruction effects on Nusselt number: ***(a)*** Nu_l - lower wall - and ***(b)*** Nu_u - upper wall.

In Fig. (8b), the case without obstruction on the upper channel wall present the highest value of the Nu_u and the other cases shows, graphically, the same values on the obstruction region. The Nu_u for asymmetric obstruction cases reveals a undershooting downstream of the obstruction. These undershooting are connected with the eddy zones behind

the inferior obstruction. The Nu_u behavior for the case with B/H = 0.4 shows an overshooting downstream of the obstruction and in sequence the undershooting. The reported overshooting is associated with the eddy zone behind the upper obstruction.

For all of the cases shown in Fig. (8), faraway of the obstruction, the Nusselt number asymptotically reaches the value predicted by the Graetz problem. In the inlet channel there is a region where the Nusselt number values are coincident for studied cases. These Nusselt behaviors indicate the regions where the obstruction effects are not relevant.

5. Conclusions

The present study shows the influence of asymmetric rectangular obstructions on the thermal and fluid dynamical entrance regions inside parallel plate channels, by taking into account the conjugate heat transfer problem with the obstructions. The obtained results were used to evaluate quantitative and qualitatively the effects of the obstruction asymmetry on the flow and temperature fields. Results show that variations of these geometric conditions have strong influence on the *momentum* and energy transfer mechanisms.

The eddy zones are associated with the coldest zones inside the channel and with the oscillation on the Nusselt number values downstream of the obstruction. There is a connection between the length of the eddy zone and the asymmetry of the obstruction. Furthermore, increasing the obstruction asymmetry the hottest region is held in shorter lengths of the channel.

6. References

Anderson, D.A., Tannehill, J.C. and Pletcher, R.H., 1984, "Computational Fluid Mechanics and Heat Transfer", Ed. Hemisphere Publishimg Corporation, New York, USA.

Andrade, C.R. and Zaparoli, E.L., 1999, "Occurrence of Reverse Heat Flux in Conjugated Heat Transfer in Finned Concentric Tubes", Proceedings of the 15th Brazilian Congress of Mechanical Engineering, CD-ROM, Rio de Janeiro, Brazil.

Caldeira, A. B., Rodrigues, R.C. and Leiroz, A., J. K., 2001, "Orifice Plate Effects On Hydrodynamical and Thermal Entrance Regions Inside Flat Channels", Proceedings of the 16th Brazilian Congress of Mechanical Engineering, CD-ROM, Uberlândia, Brazil, pp. 285-292.

Caldeira, A. B., Leiroz, A. J. K., Orlande, H. R. B., 2002, "Rectangular Obstruction Thermal Effects on Entrance Regions of Flat Plate Cahnnels", Proceedings of the 9th Brazilian Congress of Thermal Engineering and Sciences, CD-ROM, Caxambú, Brazil.

Davallah, J. and Bayazitoglu, Y, 1987, "Forced Convection Cooling Across Rectangular Blocks", J. Heat Trans. ASME, Vol. 109, pp. 321-328.

Desrayaud, G., Fichera, A. and Lauriat, G., 2002, "Conjugate Heat Transfer from a Substrate-Mounted Protruding Heat Source in Air-Cooled Vertical Channels", Proceedings of the 12th International Heat Transfer Conference, CD-ROM, Grenoble, France.

Esquiva-Dano, I., Nguyen, H. T. and Escudie, D., 2001, "Influence of Bluff-body's Shape on the Stabilization Regime of Non-premixed Flames", Combustion and Flame, Vol. 127, n 4, pp. 2167-2180.

Hanff, E. H. and Campbell, I. G., 2002, "Velocity Field Bimodality in Axisymmetric Diffusion Flame Combustor", Proceedings of the 12th International Heat Transfer Conference, CD-ROM, Grenoble, France.

Holman, J.P., 1989, "Experimental Methods for Engineers", Ed. McGraw-Hill, Singapore, Singapore.

Kays, W.M. and Crawford, M.E., 1980, "Convective Heat and Mass Transfer", 2º ed., Ed. McGraw-Hill.

Kern, D. Q., 1965, "Process Heat Transfer", Ed. McGraw-Hill, Singapore, Singapore.

Press, W. H., Teukolsky, S. A., Vetterling, W. T., Flannery, B. P., 1992, Numerical Recipes in Fortran – The Art of Scientific Computing, 2 ed, Cambridge.

Raithby, G. D., Torrance, K. E., 1974, "Upstream-Weighted Differencing Schemes and Their Application to Elliptic Problems Involving Fluid Flow", Computers & Fluids, v. 2, pp.191-206.

Versteeg, H. K. and Malalasekera, W., 1995, "An Introduction to Computational Fluid Dynamics", Ed. Prentice Hall.

Weeb, R.L., Eckert, E.R.G. and Goldstein, R.J., 1971, "Heat Transfer and Friction in Tubes with Repeated-Rib Roughness", Int. J. of Heat Mass Transfer, Vol. 14, pp. 601-617.

Williams, F. A. , 1985, "Combustion Theory", 2nd ed., Ed. Adison Wesley, USA.

Yuan, Z., Tao, W. and Wang, Q., 1998, "Numerical Prediction for Laminar Forced Convection Heat Transfer in Parallel plate channels with Streamwise-periodic Rod disturbances", Int. J. for Num. Methods in Fluids, Vol. 28, No 9, pp. 1371-1387.